NeuroImage: Clinical 18 (2018) 744–752

Contents lists available at ScienceDirect

NeuroImage: Clinical

journal homepage: www.elsevier.com/locate/ynicl

Hemispheric brain asymmetry differences in youths with attention-deficit/hyperactivity disorder

P.K. Douglas[a,b,*], Boris Gutman[c], Ariana Anderson[b], C. Larios[a], Katherine E. Lawrence[d], Katherine Narr[d], Biswa Sengupta[e], Gerald Cooray[e], David B. Douglas[f], Paul M. Thompson[c], James J. McGough[b], Susan Y. Bookheimer[b]

[a] University of Central Florida, IST, Modeling and Simulation Department, FL, USA
[b] Semel Institute for Neuroscience and Human Behavior, David Geffen School of Medicine, UCLA, CA, USA
[c] Imaging Genetics Center, USC Keck School of Medicine, Marina del Rey, CA, USA
[d] Laboratory of Neuroimaging, UCLA, CA, USA
[e] Wellcome Trust Centre for Neuroimaging, 12 Queen Square, UCL, London, UK
[f] Nuclear Medicine and Molecular Imaging, Stanford University School of Medicine, Palo Alto, CA, USA

ABSTRACT

Introduction: Attention-deficit hyperactive disorder (ADHD) is the most common neurodevelopmental disorder in children. Diagnosis is currently based on behavioral criteria, but magnetic resonance imaging (MRI) of the brain is increasingly used in ADHD research. To date however, MRI studies have provided mixed results in ADHD patients, particularly with respect to the laterality of findings.

Methods: We studied 849 children and adolescents (ages 6–21 y.o.) diagnosed with ADHD ($n = 341$) and age-matched typically developing (TD) controls with structural brain MRI. We calculated volumetric measures from 34 cortical and 14 non-cortical brain regions per hemisphere, and detailed shape morphometry of subcortical nuclei. Diffusion tensor imaging (DTI) data were collected for a subset of 104 subjects; from these, we calculated mean diffusivity and fractional anisotropy of white matter tracts. Group comparisons were made for within-hemisphere (right/left) and between hemisphere asymmetry indices (AI) for each measure.

Results: DTI mean diffusivity AI group differences were significant in cingulum, inferior and superior longitudinal fasciculus, and cortico-spinal tracts ($p < 0.001$) with the effect of stimulant treatment tending to reduce these patterns of asymmetry differences. Gray matter volumes were more asymmetric in medication free ADHD individuals compared to TD in twelve cortical regions and two non-cortical volumes studied ($p < 0.05$). Morphometric analyses revealed that caudate, hippocampus, thalamus, and amygdala were more asymmetric ($p < 0.0001$) in ADHD individuals compared to TD, and that asymmetry differences were more significant than lateralized comparisons.

Conclusions: Brain asymmetry measures allow each individual to serve as their own control, diminishing variability between individuals and when pooling data across sites. Asymmetry group differences were more significant than lateralized comparisons between ADHD and TD subjects across morphometric, volumetric, and DTI comparisons.

1. Introduction

Attention-deficit/hyperactivity disorder (ADHD) is among the most common child-onset neurodevelopmental disorders worldwide, with an estimated childhood prevalence of ~5% (Swanson et al., 1998; Wolraich et al., 1996), and an economic burden estimated in the tens of billions of dollars per year (Pelham et al., 2007). Children with ADHD have problems with task prioritization (Qiu et al., 2011), and are more likely to have emotional problems including anxiety and depression. Adolescents with ADHD are at greater risk for automobile accidents, drug experimentation, and nicotine dependency (Schubiner, 2005).

Despite copious research, many aspects of the disease pathophysiology remain unknown. Furthermore, there is a large degree of behavioral heterogeneity within the diagnosis. Traditionally, the ADHD phenotype has been characterized along the domains of inattention, hyperactivity/impulsivity or a combination of both. In children,

* Corresponding author at: University of California, 760 Westwood Blvd, Los Angeles, CA 90024, USA.
E-mail address: pamelita@g.ucla.edu (P.K. Douglas).

https://doi.org/10.1016/j.nicl.2018.02.020
Received 20 February 2017; Received in revised form 16 February 2018; Accepted 21 February 2018
Available online 24 February 2018

Table 1
Study Cohort Demographics.
Table 1. Summary of subject data for typically developing (TD), ADHD, and medication free ADHD participants by participating site. Medication free means no prior history of medication treatment for ADHD. Structural MRI data was included from the following sites: the Johns Hopkins Kennedy Krieger Institute (KKI), New York University (NYU), Oregon Health and Science University (OHSU), Peking University, and with diffusion tensor imaging (DTI) data from the University of California, Los Angeles (UCLA). Total indicated the total number of participants from that site. Female indicates the subset number, which were female. The medication free ADHD numbers reflect the subset of the total number of ADHD subjects that were medication naïve at the time of scanning. Handedness represents the percentage of subjects that were right handed. The subset number of ADHD subjects with comorbid oppositional defiant disorder (ODD) is also shown.

Diagnosis	Measure	Peking	KKI	NeuroImage	NYU	OHSU	Pittsburgh	WashU	UCLA
Typically developing									
	Total	116	61	23	99	42	89	61	17
	Female	45	27	12	52	24	43	28	11
	Age	11.7 ± 1.7	10.3 ± 1.3	17.3 ± 2.6	12.2 ± 3.1	8.9 ± 1.2	15.1 ± 2.9	11.5 ± 3.9	13.2 ± 2.0
	IQ	118.2 ± 13.3	111.5 ± 10.3	NR	110.4 ± 14.3	118.4 ± 12.6	109.8 ± 11.5	116.1 ± 14.1	110.4 ± 13.1
	Handedness	99.1	93.4	91.3	91.9	100.0	95.5	100.0	100.0
ADHD									
	Total	78	22	25	123	37	0	0	56
	Female	7	10	5	27	11	n/a	n/a	17
	Age	12.4 ± 2.0	10.2 ± 1.6	16.7 ± 2.9	11.1 ± 2.7	8.8 ± 1.0	n/a	n/a	12.6 ± 3.2
	IQ	105.4 ± 13.2	106.0 ± 15.2	NR	106.3 ± 14.3	108.5 ± 13.9	n/a	n/a	106.2 ± 13.1
	Handedness	97.4	90.1	96.0	97.6	100.0	n/a	n/a	NR
	ODD	25	6	NR	5	4	n/a	n/a	27
ADHD medication free									
	Total	52	16	NR	32	20	n/a	n/a	29
	Female	6	7	NR	10	5	n/a	n/a	8
	Age	12.7 ± 1.9	10.6 ± 1.6	NR	10.2 ± 2.3	8.8 ± 0.7	n/a	n/a	12.6 ± 3.8
	IQ	104.0 ± 12.4	107.9 ± 14.7	NR	106.9 ± 13.5	108.6 ± 13.8	n/a	n/a	106.1 ± 13.9
	Handedness	98.1	93.8	NR	96.6	100.0	n/a	n/a	NR
	ODD	14	4	NR	2	4	n/a	n/a	0

diagnosis typically is made by integrating clinical information derived from parents and teachers, and standardized ratings of ADHD presentations (McGough and McCracken, 2000). Diagnosis also hinges on the degree to which these persistent behavioral traits interfere with daily life in multiple settings including school, home, and/or work. A quantitative biomarker for the disease would be highly beneficial for diagnostic and therapeutic assessments.

Over the past decade, high-resolution magnetic resonance imaging (MRI) and diffusion tensor imaging (DTI) have been increasingly used to study anatomic differences in the ADHD brain. Nonetheless, imaging studies thus far have yielded varied results (Narr et al., 2009). For example, recent meta-analyses of structural differences report global gray matter reduction in basal ganglia regions including: caudate, putamen, and globus pallidus (Ellison-Wright et al., 2008) as well as right lentiform nucleus with mixed findings with respect to laterality (Nakao et al., 2011). A recent mega analysis found smaller volumes in accumbens, amygdala, caudate, hippocampus, putamen and intracranial volume without significant changes in pallidum (Hoogman et al., 2017). Similarly, both the laterality and significance of DTI results have varied across studies (for review, see van Ewijk et al., 2012). Interestingly, structural brain signatures of ADHD appear to resolve to some extent over the course of development (Larisch et al., 2006; Castellanos and Proal, 2009), and with stimulant treatment that enhances dopamine (DA) signaling (Shaw et al., 2009b).

Here, we hypothesized that patterns of hemispheric asymmetry differences would be observed across structural neuroimaging measures in the ADHD population. To investigate this, we studied a large cohort of ADHD youths and age-matched typically developing (TD) participants using MRI and DTI imaging techniques to assess both within hemisphere measures, and asymmetries in brain volume, morphology, and white matter microstructure.

2. Methods

2.1. Study population

We used two sources of data for this investigation. The first data set included the publicly shared ADHD200 database. These data were collected as part of the Functional Connectomes Project (FCP) and the International Neuroimaging Data sharing Initiative (INDI) (Biswal et al., 2010) as part of a push for accelerated sharing of data and analytic resources in the imaging community (Milham, 2012). We used structural MRI data collected at eight participating sites from 776 individuals (491 TD, 285 ADHD, ages 7–21 years old). The demographic data included: age, sex, full-scale IQ, and handedness, any secondary diagnosis and medication status. Adolescents in the ADHD group met criteria for ADHD on the DICA-IV and had a T-score of 65 or greater on the Conners' Parent Rating Scale (CPRS-R) long form (DSM IV inattentive), or M (DSM IV hyperactive/impulsive), or met criterion on the DuPaul ADHD Rating Scale IV (six out of nine measures marked 2, or 3 for inattentive or hyperactive/impulsivity).

The second source of data included structural MRI and DTI data collected at UCLA. A total of 104 subjects (age 6–18 y.o.) participated in this study, approved by the UCLA Institutional Review Board, (see (Lawrence et al., 2013) for further detail). All children were evaluated for ADHD and other psychiatric diagnoses based on an interview with the primary caretaker, using a semi-structured diagnostic interview, the Kiddie-Schedule for Affective Disorders and Schizophrenia–Present and Lifetime version (K-SADS-PL) and a direct interview with the child if 8 years of age or older. Parents completed the Behavior Rating Inventory of Executive Function (BRIEF), and parental ratings on the Swanson, Nolan, and Pelham, Version IV (SNAP-IV) Rating Scale were used to supplement the diagnostic interviews. A total of 56 participants met diagnostic criteria for ADHD. Controls across all data sources did not meet diagnostic criteria for ADHD or any other current psychiatric disorder.

2.2. Inclusion criteria

Psychostimulant medication can alter brain structure; therefore, subjects in the ADHD200 study whose medication history was unspecified were excluded from further analysis. Three of the sites in the ADHD200 cohort did not report medication status; therefore subjects who met diagnostic criteria for ADHD from these sites were excluded

Table 2
Cortical Gray Matter Volumetric Results Typically Developing vs. ADHD-Free.
Table 2. P-values shown for the comparison of Typically Developing (TD) individuals versus ADHD participants with no prior history of medication treatment (ADHD-Free). Comparisons include: TD Right versus ADHD-Free Right hemisphere (Right), TD Left verses ADHD-Free Left Hemisphere (Left), and the group comparison for both directional Asymmetry Index (AI) and absolute Asymmetry Index (abs(AI)) for MRI Gray Matter volume comparisons from cortical regions. *P*-values shown have been corrected for multiple comparisons, with significant comparisons shown in bold, and a + sign indicating the measure to be larger in the ADHD-Free group.

Region	Gray matter volume	Right	Left	AI	Abs(AI)
Cingulate	Caudal anterior cingulate	0.367	0.444	0.205	0.092
	Caudal middle frontal	0.334	0.231	0.763	**0.011** +
	Isthmus cingulate	0.425	0.448	0.333	**0.034** +
	Posterior cingulate	0.429	0.334	0.266	**0.024** +
	Rostral anterior cingulate	0.448	0.464	0.859	0.152
Frontal	Lateral orbito-frontal	0.367	0.402	0.961	0.250
	Medial orbitofrontal	0.488	0.402	0.830	**0.019**
	Paracentral	0.219	0.345	0.656	0.070
	Pars opercularis	0.5	0.137	0.311	0.052
	Pars orbitalis	0.334	0.476	0.242	0.384
	Pars triangularis	0.24	0.148	0.467	**0.002**
	Rostral middle frontal	**0.03** +	0.185	0.854	0.088
	Superior frontal	**0.045**	**0.032**	0.911	0.053
	Frontal pole	0.364	0.371	0.590	**0.024**
Occipital	Cuneus	0.386	0.429	0.972	**0.040** +
	Lateral occipital	0.078	0.472	0.323	**0.019** +
	Lingual	0.275	0.349	0.811	0.056
	Pericalcarine	0.492	0.464	0.606	0.132
Parietal	Inferior parietal	0.306	**0.041** +	0.649	**0.013**
	Postcentral	0.074	0.375	0.676	0.131
	Precentral	0.371	0.429	0.612	0.067
	Precuneus	0.135	0.295	0.686	**0.042** +
	Superior parietal	0.228	0.437	0.562	**0.043** +
	Supramarginal	0.425	0.262	0.581	0.118
Temporal	Entorhinal	0.413	0.456	0.588	**0.015** +
	Fusiform	0.285	0.313	0.882	0.220
	inferior temporal	0.085	**0.004** +	0.363	0.096
	Middle temporal	0.084	0.071	0.642	0.265
	Superior temporal	0.155	0.382	0.345	0.195
	Temporal Pole	0.484	0.46	0.455	0.442
	Transverse temporal	0.334	0.364	0.952	0.191
	Parahippocampal	0.448	0.398	0.533	0.108
Insulary cortex	Insula	0.356	0.386	0.956	0.087

Table 3
Subcortical MRI P-Values for Typically Developing vs. ADHD-Free.
Table 3 P-values shown for the comparison of Typically Developing (TD) individuals versus ADHD participants with no prior history of medication treatment (ADHD-Free). Comparisons include: TD Right versus ADHD-Free Right hemisphere (Right), TD Left verses ADHD-Free Left Hemisphere (Left), and the group comparison for both directional Asymmetry Index (AI) and absolute Asymmetry Index (abs(AI)). All *p*-values have been corrected for multiple comparisons. All significant, corrected *p*-values are shown in bold, with at + sign indicating larger in the ADHD-Free group.

	Right	Left	AI	Abs(AI)
Nuclues accumbens	0.982	0.984	0.804	0.216
Amygdala	0.955	0.968	0.488	**0.011** +
Caudate	0.978	0.976	0.494	0.737
Cerebellum-cortex	< **0.01** +	**0.008** +	0.944	0.652
Cerebellum white matter	0.583	0.760	0.946	0.294
Hippocampus	0.899	0.860	0.740	0.341
Inferior lateral ventricle	0.963	0.970	**0.032** + + +	**0.015**
Lateral ventricle	0.959	0.760	0.350	0.351
Pallidum	0.873	0.930	**0.015**	0.717
Putamen	0.937	0.970	0.407	0.996
Thalamus	0.793	0.970	0.553	0.252
Ventral DC	0.922	0.960	0.982	0.474
Vessel	0.965	0.980	0.205	0.358
Choroid Plexus	0.982	0.984	0.804	0.426

from the present analysis. Three TD subjects and four ADHD subjects that were included had subthreshold anxiety. However, subjects who met diagnostic criteria for any major psychiatric illness were also removed from analysis. In total, 849 participants met inclusion criteria, including 508 TD and 341 ADHD individuals. For those subjects who had a history of pharmaceutical treatment for ADHD, there was no information with respect to specific type of medication(s), dosage, or duration (for further details, see limitations section below). Therefore, we further divided ADHD subjects into two groups: subjects with a prior history of pharmacotherapy for ADHD (ADHD-Rx), and subjects who were medication naïve and therefore had no prior history of taking medication for ADHD (ADHD-Free).

2.3. MRI studies

High-resolution structural volumetric brain MRIs were collected (at 3 Tesla) according to a standardized protocol for each participant. T1-weighted MPRAGE anatomical MRI scans were processed with FreeSurfer's *recon-all* processing pipeline for whole brain segmentation and automated parcellation (Fischl and Dale, 2000). This generates segmentations for white matter, gray matter, and subcortical volumes. A mesh model of the cortical surface was then divided into 34 cortical brain regions, and for 14 subcortical and non-cortical regions per hemisphere. Total volume (mm^3) for each region was used for group comparisons.

To obtain an even more detailed description of morphometry, we applied a medial curve technique, recently developed by our group (Gutman et al., 2012). In this technique, analysts who are unaware of the clinical assessments of the subjects manually traced a region of interest for a subset of subjects randomly selected from each group ($n = 8$), until the spatial cross correlation of the shape, upon repeated tracings, is > 95%. These traces, consisting of multiple brain slices fully covering the three-dimensional anatomical structure, were extracted using an inverse-consistent fluid registration with a mutual information fidelity term to align the set of hand-labeled anatomical shape templates to each scan. The template surfaces were registered as a group following a medial-spherical registration process for each right and left hemisphere group average shape. Distances from the exterior of the shape to points along the medial curve were then calculated for each subject and used to generate statistics, which can be then mapped back on the to group shape. We applied this technique to regions frequently reported to vary in the ADHD brain including: the caudate nucleus, amygdala, hippocampus, and thalamus (Ellison-Wright et al., 2008). To study the between hemisphere asymmetry using this morphology analysis, a single group average shape was calculated by applying the medial-spherical registration process from one hemisphere onto the other in order to create a single average shape across both hemispheres and across all subjects. Because this latter process is highly computationally burdensome, we applied it to the caudate, since the caudate volume is frequently reported to vary, and because ADHD subjects have diminished levels of dopamine (DA) transporter densities in caudate regions (McGough, 2012).

2.4. Tractography analysis

All DTI data were acquired at UCLA using single-shot spin-echo/echo-planar imaging sequences with 64 non-collinear diffusion encoding directions and a 2 mm isotropic voxel size in 50 axial- oblique slices with whole brain coverage. We calculated mean diffusivity (MD), fractional anisotropy (FA), axial diffusivity (AD), and radial diffusivity (RD) for seven tracts for each hemisphere. DTI data processing was performed within the LONI Pipeline environment (Rex et al., 2003). Three-dimensional tract reconstruction was performed using a deterministic streamline approach in DTIStudio (Jiang et al., 2006) and the Fiber Assignment by Continuous Tracking (FACT) algorithm. See (Lawrence et al., 2013) for further details.

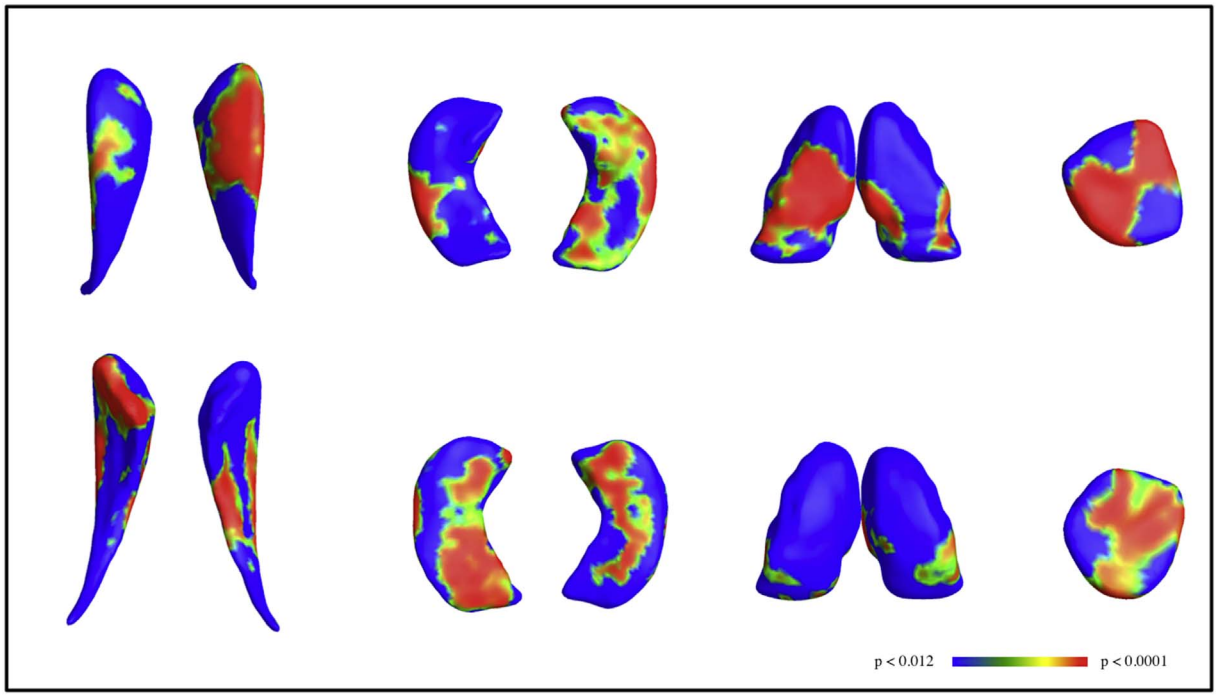

Fig. 1. (From left to right) Morphometry results for caudate, hippocampus, thalamus, and amygdala with dorsal and ventral views shown in the upper and lower panels, respectively. For each shape, the three dimensional anatomical structure is combined across subjects to create an average anatomical model for each left and right subcortical shape. Differences were computed between ADHD-Free and TD for each hemisphere. The *p*-values shown have been mapped onto their associated location for group average templates for each anatomical shape and thresholded from $p < 0.012$ (blue) to $p < 0.0001$, based on cumulative distribution functions, where red indicates increased asymmetry in the ADHD group.

2.5. Statistical analysis

For each MRI volumetric and DTI measure, we first computed within-hemisphere statistics for group comparisons (e.g., TD right hemisphere caudate volume versus ADHD right hemisphere caudate volume). To assess brain inter-hemispheric symmetry differences between ADHD and TD populations for each structural parameter (i), we calculated the asymmetry index (AI) between the left (L) and right (R) hemispheres for each subject (j) as:

$$AI_{ij} = \frac{L_{ij} - R_{ij}}{\mu_{ij}}$$

where μ is the mean value across hemispheres (Steinmetz et al., 1990). We hypothesized that hemispheric asymmetry differences may vary in their lateralization. We therefore additionally assessed differences in the absolute value of the AI between subject populations. Crucially, this method allows individual brains to serve as their own anatomic control, diminishing the influence of inter-site variability.

We used a general linear mixed effects model to study the relationship between within-hemisphere and AI differences in ADHD (Bates et al., 2012). Fixed effects included: site of data collection, age, sex, diagnosis, and their interactions, to account for known differences in maturation rates in the ADHD population (Larisch et al., 2006; Castellanos and Proal, 2009). *P*-values were obtained by likelihood ratio tests of the full model against the null-model that disregarded the influence of diagnosis. All code for this analysis was implemented in the language "R", using the linear mixed-effects *lme* model tool (Bates et al., 2012). All reported *p*-values were adjusted to correct for multiple comparisons (Benjamini and Hochberg, 1995) within our code. Participant ID was included as a random effect within the model to account for multiple comparisons.

For our morphology analysis, statistical tests consisted of computing overall p-values for group differences along the medial curve based on permutation tests (100,000 iterations), and based on the standardized method for this protocol (Thompson et al., 2004). We also computed cumulative distribution functions as a way to visualize the relationship between the statistical threshold and the extent of the effect.

3. Results

3.1. Study cohort characteristics

The mean age of TD and ADHD participants included in the analysis was 12.1 ± 3.2 and 11.6 ± 2.3 years old with 45% and 29% of females, respectively. The average full scale IQ was 110.8 ± 12.2 for TD individuals, and 113.8 ± 12.8 for ADHD individuals. Of the participants who met diagnostic criteria for ADHD, 26% had comorbid oppositional defiant disorder. Table 1 summarizes the diagnostic, demographic, and medication status information across study cohorts for subjects included in the analysis.

3.2. Brain asymmetry and neuroimaging findings

After adjustment for age, sex, and site we observed statistically significant cortical gray matter differences for group comparisons between TD and ADHD-free subjects in lateralized comparisons including: rostral middle and superior frontal regions in the right hemisphere, and superior frontal, inferior parietal, and inferior temporal regions in the left hemisphere. AI did not reveal any significant changes between TD and ADHD-free groups in cortical gray matter volumes. In contrast, the absolute AI was significantly different in eleven cortical gray matter volumes with a focus in cingulate and parietal regions after correction for multiple comparisons (Table 2). In all of these comparisons, the mean absolute magnitude of AI was increased in ADHD compared to TD subjects. Results for cortical gray matter volume comparisons between TD and ADHD-Rx as well as ADHD-Rx and ADHD-Free groups are summarized in Supplementary Table 1. For the TD versus ADHD-Rx comparison, lateral occipital AI was significant, and only one absolute AI comparison was significant. When comparing ADHD individuals who had prior exposure to pharmaceutical treatment for ADHD (ADHD-Rx)

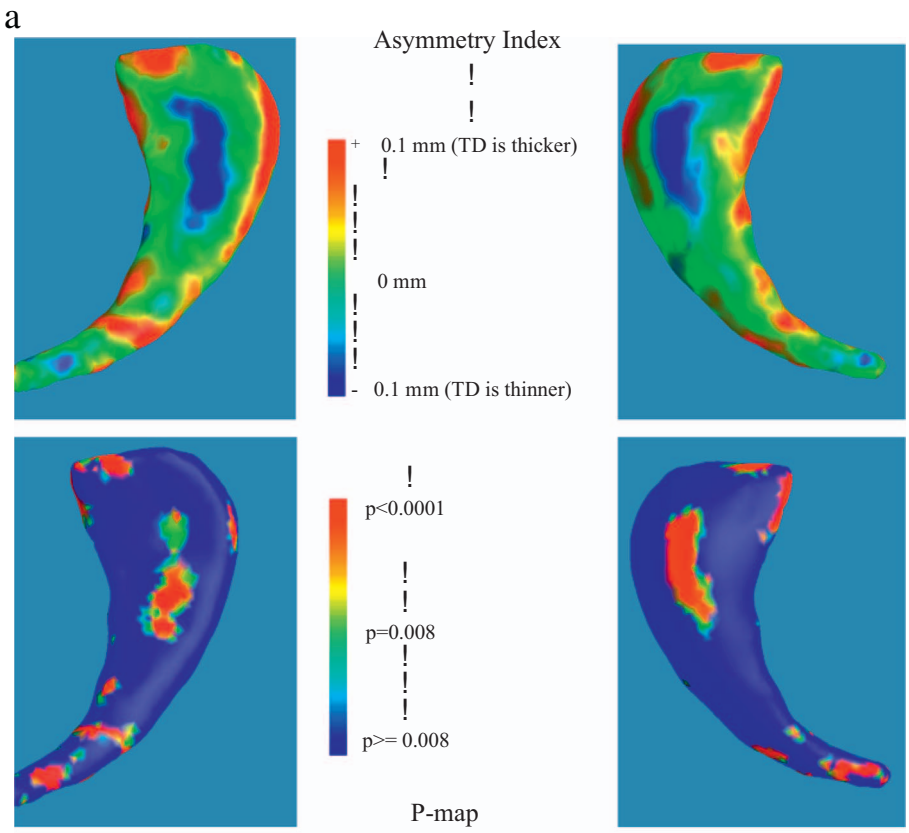

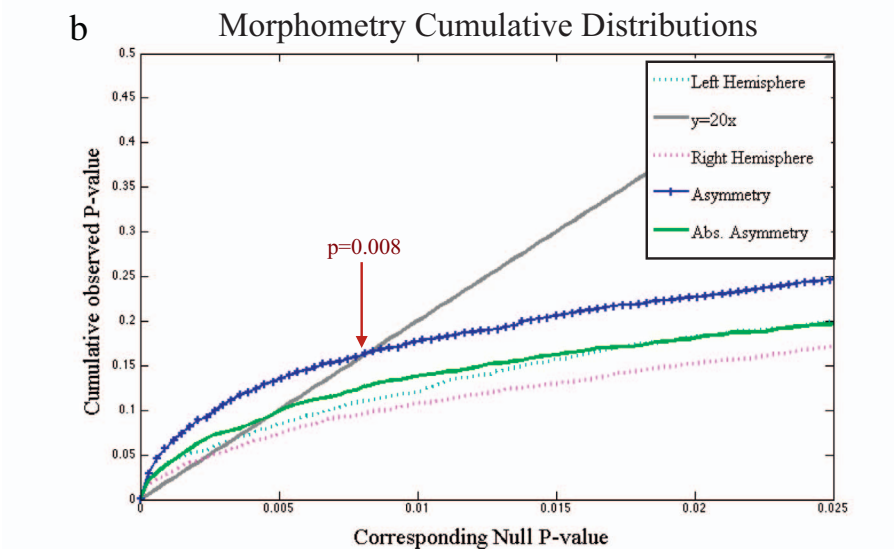

Fig. 2. a. Morphometry results for Caudate Asymmetry Index shown for thickness differences (top) and associated p-maps (bottom). Note the critical q-value used to threshold the p-maps was derived from the cumulative distribution function for Asymmetry, shown in Fig. 2b. Here, all morphology changes were mapped onto the group average shape, calculated using all caudates from both hemispheres. **b.** Cumulative distribution functions (CDFs) calculated across morphology results for the ADHD Left versus Typically Developing (TD) Left Caudate (turquoise), ADHD Right versus TD right caudates (magenta), and both Asymmetry (blue) and absolute Asymmetry (green). The q-value, or point along the x-axis that corresponds to the intersection of the CDF and y = 20x line other than the origin, is a measure of the overall significance of the p-value maps. The q-value of the CDF for both symmetry indices were higher than q-values for either right or left CDFs, suggesting that this analysis method boosts the statistical power to detect group morphology differences between TD and ADHD subjects.

with those with no prior medication exposure (ADHD-Free), only postcentral parietal and temporal pole absolute AI showed significantly different volumes.

We performed these same comparisons for subcortical volumes. The cerebellar cortex was significantly different with both left and right within-hemisphere comparisons. Both asymmetry comparisons revealed differences in inferior lateral ventricle. Differences in pallidum and amygdala were significant for AI and absolute AI comparisons respectively (Table 3). Inferior lateral ventricle differences were significant in all asymmetry evaluations when comparing the ADHD-Rx group with either the TD or ADHD-free group (Supplementary Table 2). Distribution plots showing differences in AI based on volumetric results for TD, medication free ADHD, and subjects with a history of stimulant treatment for ADHD are shown in Supplementary Fig. 1.

Morphology p-map results are shown in Fig. 1 for the caudate, thalamus, hippocampus, and amygdala for lateralized comparisons between the TD and ADHD-free groups. Morphologic changes in the caudate appeared to be localized primarily to the head region for both lateralized (Fig. 1) and AI (Fig. 2) morphological thickness differences, consistent with known anatomic connectivity of this caudate region to frontal executive areas that are also altered structurally in ADHD individuals. The cumulative distribution function (CDF) of the *p*-values is commonly generated when applying false discovery rate methods to assign overall significance values to statistical maps, and can be used to

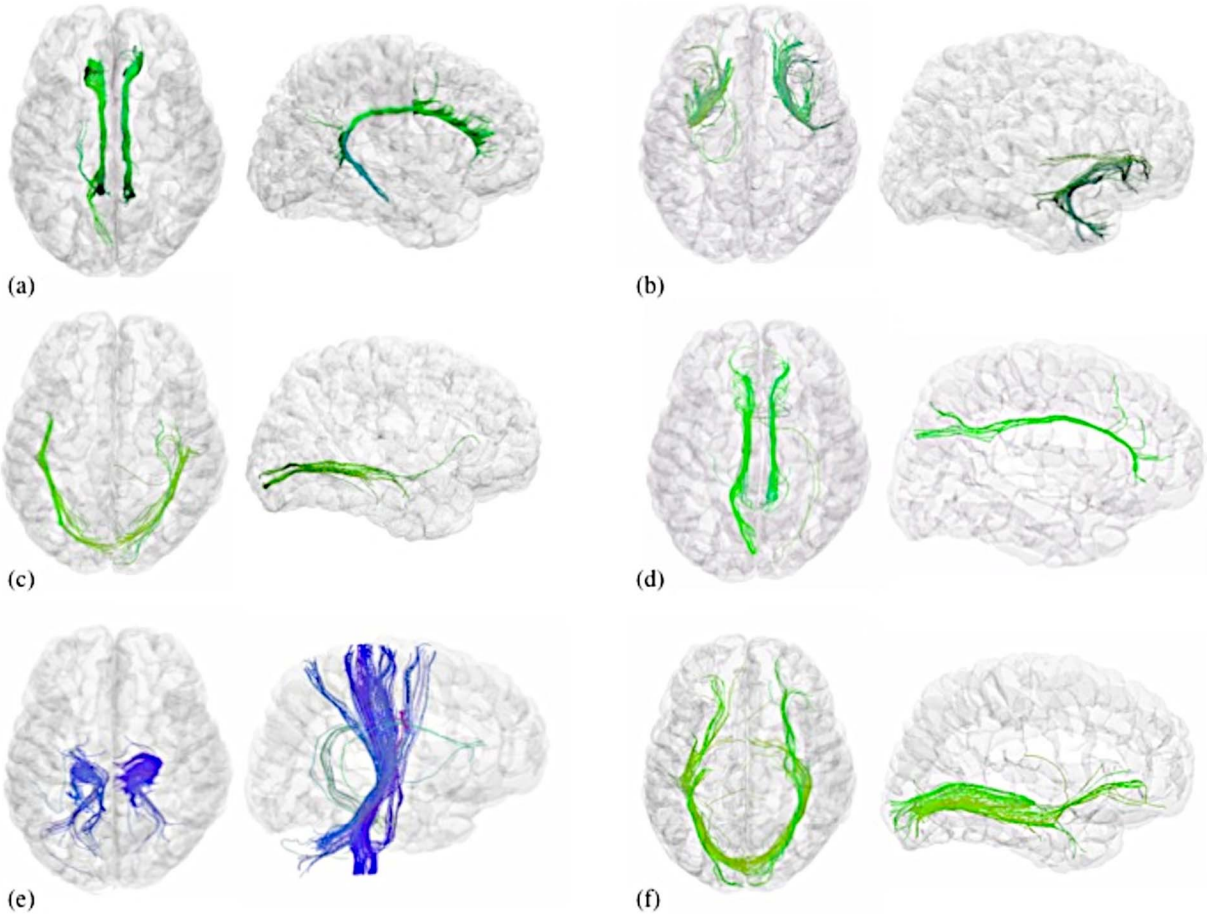

Fig. 3. Illustrative figure of tractography fibers that showed significant differences between ADHD-Free and TD groups. Axial and sagittal views shown for (a) cingulum, (b) uncinate fasciculus, (c) inferior longitudinal fasciculus, (d) superior longitudinal fasciculus, (e) corticospinal tract, and (f) inferior fronto-occipital fasciculus. All images created were created using DTI data from BrainSuite version 14c with 0.5 track seeds per voxel (Yan et al., 2011; Shattuck et al., 2009) using region of interest locations specified in (Catani, 2006) and 20 mm spheres. Colors indicate the average of the directions along the fiber tracts as follows: green (anterior/posterior), blue (inferior/superior).

compare the power of different methods applied to the same set of images (Hua et al., 2009). The q-value, or intersection with of the CDF with the y = 20x line, reflects the overall significance of each p-value map. Fig. 2b shows CDFs calculated for morphometric measures for ADHD right versus TD right hemisphere, ADHD left verses TD left, and AI comparisons. Asymmetry differences resulted in higher q-values than absolute asymmetry, and both q-values were higher than right and left hemispheric morphology comparisons.

After adjustment for age and sex, significant differences in AI were found in certain measures in six white matter tracts, and absolute AI in seven white matter tracts (Fig. 3). FA asymmetry differences were found in the uncinate fasciculus, cingulum, and corticospinal tract. Hemispheric differences in radial (perpendicular) diffusivity were noted in the inferior longitudinal fasciculus (ILF), cingulum, superior longitudinal fasciculus (SLF), and corticospinal tract. Symmetry differences in axial (parallel) diffusivity were noted in uncinate, cingulum, ILF, and SLF. Increased disease severity on the Inattention scale was associated with increased brain asymmetry in the lateral orbito-frontal gray matter volume. Increased hyperactivity and inattention scores were correlated with increased asymmetry in fusiform cortex. In contrast, there were no significant DTI results for within-hemisphere group comparisons in the right hemisphere. Left hemisphere differences were significant in inferior fronto-occipital and anterior thalamic radiation (Table 4).

There were no significant asymmetry differences between ADHD-Rx and ADHD-Free. However, significant asymmetry differences between ADHD-Rx and TD groups were observed in uncinate fasciculus, cingulum, inferior longitudinal fasciculus, superior longitudinal fasciculus, and corticospinal tract (Supplementary Table 3). Distribution plots showing differences in AI based on FA measures for TD, ADHD-Rx, and ADHD-Free are shown in Supplementary Fig. 2.

4. Discussion

Most human brains show some degree of asymmetry. Normal variation and functional specialization produce asymmetries of structure, function, and behavior that evolve throughout life, and are thought to originate from developmental, hereditary, experiential and pathological factors (Toga and Thompson, 2003). Attention itself induces functional asymmetries in healthy individuals. For example, PET and EEG studies suggest that attention directed to global aspects of visual processing is more right lateralized, but local processing is more left hemisphere dominant (Fink et al., 1996; Yamaguchi et al., 2000).

However, certain pathologies can also modulate, exacerbate, or arise from brain asymmetries (Thompson et al., 1998; Crow, 1997), including impulsivity (Gordon, 2016). In ADHD, early lesion studies suggested a role for unilateral right hemisphere dysfunction (Heilman and Van Den Abell, 1980; Stefanatos and Wasserstein, 2001). Previous studies have investigated aspects of structural brain symmetry in ADHD (Rubia et al., 2000; Hale et al., 2015; Shaw et al., 2009a). One of these studies reported *increased* asymmetry in the TD group, using homologous points on the cortex for comparison (Shaw et al., 2009a). A few of our DTI comparisons showed increased AI in the TD group (see Table 4), however all of our cortical volumetric comparisons showed

Table 4
Diffusion Tensor Imaging Results for Typically Developing versus ADHD-Free.
Table 4. Diffusion tensor imaging results for typically developing (TD) versus ADHD individuals with no history of medication treatment (ADHD-Free). Measures included: fractional anisotropy (FA), mean diffusivity (MD), radial diffusivity (RD), and axial diffusivity (AD). Results shown for the following comparisons: TD Right versus ADHD-Free Right hemisphere, (Right) TD Left verses ADHD-Free Left Hemisphere (Left), and both directional Asymmetry Index (AI) and absolute Asymmetry Index (abs(AI)) for TD and ADHD-Free groups. All reported p-values have been adjusted to correct multiple comparisons, to a false discovery rate of 0.05. All significant *p* values are shown in bold, and a + sign indicates that the value was higher in the ADHD group.

Fiber Tract	Measure	Right	Left	AI	Abs(AI)
Uncinate fasciculus	FA	0.880	0.390	**p < 0.001** +	**p < 0.001** +
	MD	0.225	0.655	0.333	**0.001**
	RD	0.303	0.487	0.542	**0.001** +
	AD	0.191	0.766	**0.001** +	**p < 0.001**
Cingulum	FA	0.618	0.596	**p < 0.001**	0.810
	MD	0.691	0.444	**p < 0.001** +	**p < 0.001**+
	RD	0.941	0.792	**p < 0.001** +	**p < 0.001**+
	AD	0.372	0.201	**0.005** +	**p < 0.001**+
Inferior longitudinal fasciculus	FA	0.785	0.816	**0.038**	0.307
	MD	0.206	0.290	**p < 0.001**+	**p < 0.001**
	RD	0.511	0.669	**p < 0.001**+	**p < 0.001**
	AD	0.107	0.093	**p < 0.001**+	**p < 0.001**
Inferior fronto-occipital	FA	0.397	0.770	**0.042** +	**0.001**
	MD	0.319	0.168	0.198	**0.039** +
	RD	0.704	0.418	0.128	0.051
	AD	0.105	**0.048**	0.412	**0.028** +
Anterior thalamic radiation	FA	0.956	0.981	0.840	0.095
	MD	0.088	**0.025** +	0.050	**p < 0.001** +
	RD	0.207	0.145	0.155	**0.002** +
	AD	0.066	**0.018**	**0.022** +	**p < 0.001**+
Superior longitudinal fasciculus	FA	0.975	0.417	**0.031**+	**0.001**+
	MD	0.197	0.305	**p < 0.001**+	**p < 0.001**
	RD	0.338	0.763	**p < 0.001**+	**p < 0.001**
	AD	0.138	0.056	**p < 0.001**+	**p < 0.001**+
Corticospinal tract	FA	0.266	0.825	**0.001**	0.435
	MD	0.345	0.262	**0.002**+	**p < 0.001**+
	RD	0.336	0.445	**0.001**+	**p < 0.001**+
	AD	0.448	0.184	**0.037**+	**0.002**

increased absolute AI in the ADHD population (see also Supplementary Fig. 1). We suggest that findings reported previously may be due to the ADHD population consisting mostly of subjects with a history of psychostimulant medication (Shaw et al., 2009a). Pathologic brain asymmetries should be considered in terms of their impact on the brain as a whole. Increased or atypical functional asymmetry and abnormal interhemispheric processing have now been reported in a number of ADHD fMRI studies (Hale et al., 2007; Fassbender and Schweitzer, 2006). The EEG P3 event-related potential is also more asymmetrically distributed in ADHD subjects (Senderecka et al., 2012; Kuperman et al., 1996). Functional asymmetry of stimulus processing (Yordanova et al., 2013) including visual and default mode networks (DMN) (Anderson et al., 2014) appears to be characteristic of the disease. Interestingly, our cortical results showed consistently increased AI in key DMN loci and lateral occipital cortex.

One implication of these results is the possibility that asymmetries in the brain's structural layout may subtend the behavioral aspects of ADHD. White matter structural changes were perhaps most striking, with increased AI in fronto-parietal circuitry. Interestingly, increased anatomic lateralization of SLF fronto-parietal connections is predictive of behavioral performance on detection time visuospatial tasks (Thiebaut de Schotten et al., 2011). The uncinate fasciculus participates with the limbic system, thought to be abnormal in ADHD (Brieber et al., 2007; Sowell et al., 2003). The IFL connects visual areas with the amygdala and hippocampus and is involved in visual perception and reading (Catani et al., 2003). The cingulum has known involvement in attentional processes (Catani, 2006), connecting frontal, parietal, temporal and occipital cortex.

Developmental differences in caudate volume maturation have been noted in childhood ADHD, and these appear to resolve to some extent during adolescence (Castellanos et al., 2002; Nakao et al., 2011). However, some degrees of volumetric reductions in caudate nucleus appear to persist into adulthood (Onnink et al., 2014; Seidman et al., 2011). Our results suggest that asymmetric maturation rates between the hemispheres may be a critical detail in understanding structural brain changes across the lifespan.

4.1. Temporal integration

Problems with task-prioritization and increased variability in reaction time (RT) are well-established behavioral traits of ADHD. Changes in fiber myelination, and axonal diameter that are reflected in DTI measurements, are correlated with conduction velocities (Alexander et al., 2007), and increased asymmetry may therefore lead to unbalanced conduction speeds. We posit that RT variability may be a reflection of improper temporal integration in processing incoming stimuli across hemispheres.

4.2. Limitations and future studies

A number of study limitations should be noted. First, the potential for cohort heterogeneity with respect to diagnosis is possible. Nonetheless, most reproducibility studies have demonstrated high inter-rater, test-retest reliability, and consistency across diagnostic metrics with respect to whether the individual has ADHD or not (e.g., Faries et al., 2001; Zhang et al., 2005). There is also likely heterogeneity with respect to the medication group (ADHD-Rx), since data was not provided with respect to dosage, type of medication, or duration.

In this work, we chose to group all subjects with ADHD without subdividing into subtypes, or referred to now in the DSM V as presentations. For some time, the extent to which these behavioral phenotypes form distinct diagnostic categories has been an issue of some debate (e.g., Woo and Rey, 2005). In the publications describing results of the ADHD200 contest, one of the consistent findings - across groups - was the ability for pattern classification algorithms to correctly make group-membership predictions at the level of ADHD from non-ADHD (or TD) with considerably high accuracy (Colby et al., 2012; Douglas et al., 2012). In comparison, the taxonomic prediction of subtype was considerably less accurate. A number of manuscripts leading up to this competition suggested a latent dimensional component to ADHD (e.g., Marcus and Barry, 2011). Our recent work building on our supervised learning work of the ADHD200 competition leveraged unsupervised non-negative matrix factorization. This work discovered clusters nominated by the data, which showed a great degree of heterogeneity with respect to the subtype label within a given cluster, thus favoring a more dimensional latent structure (see Anderson et al., 2014). Future work may further explore the extent to which archetypal clusters of ADHD as defined by neuroimaging and behavioral measures are related to disease comorbidities (e.g., ODD) and treatment response. A recent cross-sectional mega-analysis by our group and others examined structural changes across the lifespan, and found greater effect sizes in children compared to adults, supporting the delayed maturation theory for ADHD (Hoogman et al., 2017).

Psychostimulant treatment of ADHD now represents the largest single class of psychotropic medications prescribed to children in the US, and around 9% of all boys and 4% of girls will receive this medication during childhood or adolescence (Visser et al., 2014; "Centers for Disease Control and Prevention. Increasing Prevalence of Parent-Reported Attention-Deficit/Hyperactivity Disorder Among Children,", 2010). Future analyses may further examine how medication treatment alters structural changes before and after puberty and across the lifespan.

5. Conclusions

Altered patterns of hemispheric asymmetry in ADHD youths were observed across cortical and subcortical volumes, subcortical morphology and white matter microstructure. Although neuroimaging is not part of the typical diagnostic workup, this knowledge may allow us to better appreciate the spectrum of ADHD behavioral traits as they evolve through treatment and across the lifespan.

Acknowledgements

The authors would like to thank the Klingenstein Third Generation Foundation, the NIH K01 Award 1K01MH110645, the NIH/National Center for Advancing Translational Science (NCATS) UCLA CTSI Grant Number UL1TR000124, and the Brain and Behavior Research foundation for a NARSAD Young Investigator Award for their kind support of this research.

Financial disclosures

The authors have no conflicts of interest to report.

Appendix A. Supplementary data

Supplementary data to this article can be found online at https://doi.org/10.1016/j.nicl.2018.02.020.

References

Alexander, A.L., Lee, J.E., Lazar, M., Field, A.S., 2007. Diffusion tensor imaging of the brain. Neurother. J. Am. Soc. Exp. Neurother. 4, 316–329. http://dx.doi.org/10.1016/j.nurt.2007.05.011.

Anderson, A., Douglas, P.K., Kerr, W.T., Haynes, V.S., Yuille, A.L., Xie, J., Wu, Y.N., Brown, J.A., Cohen, M.S., 2014. Non-negative matrix factorization of multimodal MRI, fMRI and phenotypic data reveals differential changes in default mode subnetworks in ADHD. NeuroImage 102 (Pt 1), 207–219. http://dx.doi.org/10.1016/j.neuroimage.2013.12.015.

Bates, D., Machler, M., Bolker, B., Walker, S., 2012. Fitting linear mixed-effects models using lme4. J. Stat. Softw. 67 (1), 1–48.

Benjamini, Y., Hochberg, Y., 1995. Controlling the false discovery rate: a practical and powerful approach to multiple testing. J. R. Stat. Soc. Ser. B 57, 289–300.

Biswal, B.B., Mennes, M., Zuo, X.-N., Gohel, S., Kelly, C., Smith, S.M., Beckmann, C.F., Adelstein, J.S., Buckner, R.L., Colcombe, S., Dogonowski, A.-M., Ernst, M., Fair, D., Hampson, M., Hoptman, M.J., Hyde, J.S., Kiviniemi, V.J., Kötter, R., Li, S.-J., Lin, C.-P., Lowe, M.J., Mackay, C., Madden, D.J., Madsen, K.H., Margulies, D.S., Mayberg, H.S., McMahon, K., Monk, C.S., Mostofsky, S.H., Nagel, B.J., Pekar, J.J., Peltier, S.J., Petersen, S.E., Riedl, V., Rombouts, S.A.R.B., Rypma, B., Schlaggar, B.L., Schmidt, S., Seidler, R.D., Siegle, G.J., Sorg, C., Teng, G.-J., Veijola, J., Villringer, A., Walter, M., Wang, L., Weng, X.-C., Whitfield-Gabrieli, S., Williamson, P., Windischberger, C., Zang, Y.-F., Zhang, H.-Y., Castellanos, F.X., Milham, M.P., 2010. Toward discovery science of human brain function. Proc. Natl. Acad. Sci. U. S. A. 107, 4734–4739. http://dx.doi.org/10.1073/pnas.0911855107.

Brieber, S., Neufang, S., Bruning, N., Kamp-Becker, I., Remschmidt, H., Herpertz-Dahlmann, B., Fink, G.R., Konrad, K., 2007. Structural brain abnormalities in adolescents with autism spectrum disorder and patients with attention deficit/hyperactivity disorder. J. Child Psychol. Psychiatry 48, 1251–1258. http://dx.doi.org/10.1111/j.1469-7610.2007.01799.x.

Castellanos, F.X., Proal, E., 2009. Location, location, and thickness: volumetric neuroimaging of attention-deficit/hyperactivity disorder comes of age. J. Am. Acad. Child Adolesc. Psychiatry 48, 979–981. http://dx.doi.org/10.1097/CHI.0b013e3181b45084.

Castellanos, F.X., Lee, P.P., Sharp, W., Jeffries, N.O., Greenstein, D.K., Clasen, L.S., Blumenthal, J.D., James, R.S., Ebens, C.L., Walter, J.M., Zijdenbos, A., Evans, A.C., Giedd, J.N., Rapoport, J.L., 2002. Developmental trajectories of brain volume abnormalities in children and adolescents with attention-deficit/hyperactivity disorder. JAMA 288, 1740–1748.

Catani, M., 2006. Diffusion tensor magnetic resonance imaging tractography in cognitive disorders. Curr. Opin. Neurol. 19, 599–606. http://dx.doi.org/10.1097/01.wco.0000247610.44106.3f.

Catani, M., Jones, D.K., Donato, R., Ffytche, D.H., 2003. Occipito-temporal connections in the human brain. Brain J. Neurol. 126, 2093–2107. http://dx.doi.org/10.1093/brain/awg203.

Centers for Disease Control and Prevention, 2010. Increasing prevalence of parent-reported attention-deficit/hyperactivity disorder among children. MMWR 59, 1439–1443.

Colby, J.B., Rudie, J.D., Brown, J.A., Douglas, P.K., Cohen, M.S., Shehzad, Z., 2012. Insights into multimodal imaging classification of ADHD. Front. Syst. Neurosci. 6, 59. http://dx.doi.org/10.3389/fnsys.2012.00059.

Crow, T.J., 1997. Schizophrenia as failure of hemispheric dominance for language. Trends Neurosci. 20, 339–343.

Douglas, P., Colby, J.B., Shehzad, Z., Rudie, J.D., Brown, J.A., 2012. Multimodal classification of ADHD: combining features across domains to improve classification. OHBM 374.

Ellison-Wright, I., Ellison-Wright, Z., Bullmore, E., 2008. Structural brain change in attention deficit hyperactivity disorder identified by meta-analysis. BMC Psychiatry 8, 51. http://dx.doi.org/10.1186/1471-244X-8-51.

van Ewijk, H., Heslenfeld, D.J., Zwiers, M.P., Buitelaar, J.K., Oosterlaan, J., 2012. Diffusion tensor imaging in attention deficit/hyperactivity disorder: a systematic review and meta-analysis. Neurosci. Biobehav. Rev. 36, 1093–1106. http://dx.doi.org/10.1016/j.neubiorev.2012.01.003.

Faries, D.E., Yalcin, I., Harder, D., Heiligenstein, J.H., 2001. Validation of the ADHD rating scale as a clirlician administered and scored instrument. J. Atten. Disord. 5, 107–115. http://dx.doi.org/10.1177/108705470100500204.

Fassbender, C., Schweitzer, J.B., 2006. Is there evidence for neural compensation in attention deficit hyperactivity disorder? A review of the functional neuroimaging literature. Clin. Psychol. Rev. 26, 445–465. http://dx.doi.org/10.1016/j.cpr.2006.01.003.

Fink, G.R., Halligan, P.W., Marshall, J.C., Frith, C.D., Frackowiak, R.S., Dolan, R.J., 1996. Where in the brain does visual attention select the forest and the trees? Nature 382, 626–628. http://dx.doi.org/10.1038/382626a0.

Fischl, B., Dale, A.M., 2000. Measuring the thickness of the human cerebral cortex from magnetic resonance images. Proc. Natl. Acad. Sci. U. S. A. 97, 11050–11055. http://dx.doi.org/10.1073/pnas.200033797.

Gordon, H., 2016. Laterality of brain activation for risk factors of addiction. Curr. Drug Abuse Rev. 9, 1–18. http://dx.doi.org/10.2174/1874473709666151217121309.

Gutman, B.A., Wang, Y., Rajagopalan, P., Toga, A.W., Thompson, P.M., 2012. Shape matching with medial curves and 1-D group-wise registration. IEEE 716–719. http://dx.doi.org/10.1109/ISBI.2012.6235648.

Hale, T.S., Bookheimer, S., McGough, J.J., Phillips, J.M., McCracken, J.T., 2007. Atypical brain activation during simple & complex levels of processing in adult ADHD: an fMRI study. J. Atten. Disord. 11, 125–140. http://dx.doi.org/10.1177/1087054706294101.

Hale, T.S., Wiley, J.F., Smalley, S.L., Tung, K.L., Kaminsky, O., McGough, J.J., Jaini, A.M., Loo, S.K., 2015. A parietal biomarker for ADHD liability: as predicted by the distributed effects perspective model of ADHD. Front. Psychiatry 6, 63. http://dx.doi.org/10.3389/fpsyt.2015.00063.

Heilman, K.M., Van Den Abell, T., 1980. Right hemisphere dominance for attention: the mechanism underlying hemispheric asymmetries of inattention (neglect). Neurology 30, 327–330.

Hoogman, M., Bralten, J., Hibar, D.P., Mennes, M., Zwiers, M.P., Schweren, L.S.J., van Hulzen, K.J.E., Medland, S.E., Shumskaya, E., Jahanshad, N., de Zeeuw, P., Szekely, E., Sudre, G., Wolfers, T., Onnink, A.M.H., Dammers, J.T., Mostert, J.C., Vives-Gilabert, Y., Kohls, G., Oberwelland, E., Seitz, J., Schulte-Rüther, M., Ambrosino, S., Doyle, A.E., Høvik, M.F., Dramsdahl, M., Tamm, L., van Erp, T.G.M., Dale, A., Schork, A., Conzelmann, A., Zierhut, K., Baur, R., McCarthy, H., Yoncheva, Y.N., Cubillo, A., Chantiluke, K., Mehta, M.A., Paloyelis, Y., Hohmann, S., Baumeister, S., Bramati, I., Mattos, P., Tovar-Moll, F., Douglas, P., Banaschewski, T., Brandeis, D., Kuntsi, J., Asherson, P., Rubia, K., Kelly, C., Martino, A.D., Milham, M.P., Castellanos, F.X., Frodl, T., Zentis, M., Lesch, K.-P., Reif, A., Pauli, P., Jernigan, T.L., Haavik, J., Plessen, K.J., Lundervold, A.J., Hugdahl, K., Seidman, L.J., Biederman, J., Rommelse, N., Heslenfeld, D.J., Hartman, C.A., Hoekstra, P.J., Oosterlaan, J., von Polier, G., Konrad, K., Vilarroya, O., Ramos-Quiroga, J.A., Soliva, J.C., Durston, S., Buitelaar, J.K., Faraone, S.V., Shaw, P., Thompson, P.M., Franke, B., 2017. Subcortical brain volume differences in participants with attention deficit hyperactivity disorder in children and adults: a cross-sectional mega-analysis. Lancet Psychiatry. http://dx.doi.org/10.1016/S2215-0366(17)30049-4.

Hua, X., Lee, S., Yanovsky, I., Leow, A.D., Chou, Y.-Y., Ho, A.J., Gutman, B., Toga, A.W., Jack, C.R., Bernstein, M.A., Reiman, E.M., Harvey, D.J., Kornak, J., Schuff, N., Alexander, G.E., Weiner, M.W., Thompson, P.M., 2009. Optimizing power to track brain degeneration in Alzheimer's disease and mild cognitive impairment with tensor-based morphometry: an ADNI study of 515 subjects. NeuroImage 48, 668–681. http://dx.doi.org/10.1016/j.neuroimage.2009.07.011.

Jiang, H., van Zijl, P.C.M., Kim, J., Pearlson, G.D., Mori, S., 2006. DtiStudio: resource program for diffusion tensor computation and fiber bundle tracking. Comput. Methods Prog. Biomed. 81, 106–116. http://dx.doi.org/10.1016/j.cmpb.2005.08.004.

Kuperman, S., Johnson, B., Arndt, S., Lindgren, S., Wolraich, M., 1996. Quantitative EEG differences in a nonclinical sample of children with ADHD and undifferentiated ADD. J. Am. Acad. Child Adolesc. Psychiatry 35, 1009–1017. http://dx.doi.org/10.1097/00004583-199608000-00011.

Larisch, R., Sitte, W., Antke, C., Nikolaus, S., Franz, M., Tress, W., Müller, H.-W., 2006. Striatal dopamine transporter density in drug naive patients with attention-deficit/hyperactivity disorder. Nucl. Med. Commun. 27, 267–270.

Lawrence, K.E., Levitt, J.G., Loo, S.K., Ly, R., Yee, V., O'Neill, J., Alger, J., Narr, K.L., 2013. White matter microstructure in subjects with attention-deficit/hyperactivity disorder and their siblings. J. Am. Acad. Child Adolesc. Psychiatry 52, 431–440.e4. http://dx.doi.org/10.1016/j.jaac.2013.01.010.

Marcus, D.K., Barry, T.D., 2011. Does attention-deficit/hyperactivity disorder have a dimensional latent structure? A taxometric analysis. J. Abnorm. Psychol. 120, 427–442. http://dx.doi.org/10.1037/a0021405.

McGough, J.J., 2012. Attention deficit hyperactivity disorder pharmacogenetics: the dopamine transporter and D4 receptor. Pharmacogenomics 13, 365–368. http://dx.doi.org/10.2217/pgs.12.5.

McGough, J.J., McCracken, J.T., 2000. Assessment of attention deficit hyperactivity disorder: a review of recent literature. Curr. Opin. Pediatr. 12, 319–324.
Milham, M.P., 2012. Open neuroscience solutions for the connectome-wide association era. Neuron 73, 214–218. http://dx.doi.org/10.1016/j.neuron.2011.11.004.
Nakao, T., Radua, J., Rubia, K., Mataix-Cols, D., 2011. Gray matter volume abnormalities in ADHD: voxel-based meta-analysis exploring the effects of age and stimulant medication. Am. J. Psychiatry 168, 1154–1163. http://dx.doi.org/10.1176/appi.ajp.2011.11020281.
Narr, K.L., Woods, R.P., Lin, J., Kim, J., Phillips, O.R., Del'Homme, M., Caplan, R., Toga, A.W., McCracken, J.T., Levitt, J.G., 2009. Widespread cortical thinning is a robust anatomical marker for attention-deficit/hyperactivity disorder. J. Am. Acad. Child Adolesc. Psychiatry 48, 1014–1022. http://dx.doi.org/10.1097/CHI.0b013e3181b395c0.
Onnink, A.M.H., Zwiers, M.P., Hoogman, M., Mostert, J.C., Kan, C.C., Buitelaar, J., Franke, B., 2014. Brain alterations in adult ADHD: effects of gender, treatment and comorbid depression. Eur. Neuropsychopharmacol. J. Eur. Coll. Neuropsychopharmacol. 24, 397–409. http://dx.doi.org/10.1016/j.euroneuro.2013.11.011.
Pelham, W.E., Foster, E.M., Robb, J.A., 2007. The economic impact of attention-deficit/hyperactivity disorder in children and adolescents. J. Pediatr. Psychol. 32, 711–727. http://dx.doi.org/10.1093/jpepsy/jsm022.
Qiu, M., Ye, Z., Li, Q., Liu, G., Xie, B., Wang, J., 2011. Changes of brain structure and function in ADHD children. Brain Topogr. 24, 243–252. http://dx.doi.org/10.1007/s10548-010-0168-4.
Rex, D.E., Ma, J.Q., Toga, A.W., 2003. The LONI pipeline processing environment. NeuroImage 19, 1033–1048.
Rubia, K., Overmeyer, S., Taylor, E., Brammer, M., Williams, S.C., Simmons, A., Andrew, C., Bullmore, E.T., 2000. Functional frontalisation with age: mapping neurodevelopmental trajectories with fMRI. Neurosci. Biobehav. Rev. 24, 13–19.
Schubiner, H., 2005. Substance abuse in patients with attention-deficit hyperactivity disorder: therapeutic implications. CNS Drugs 19, 643–655.
Seidman, L.J., Biederman, J., Liang, L., Valera, E.M., Monuteaux, M.C., Brown, A., Kaiser, J., Spencer, T., Faraone, S.V., Makris, N., 2011. Gray matter alterations in adults with attention-deficit/hyperactivity disorder identified by voxel based morphometry. Biol. Psychiatry 69, 857–866. http://dx.doi.org/10.1016/j.biopsych.2010.09.053.
Senderecka, M., Grabowska, A., Gerc, K., Szewczyk, J., Chmylak, R., 2012. Event-related potentials in children with attention deficit hyperactivity disorder: an investigation using an auditory oddball task. Int. J. Psychophysiol. 85, 106–115. http://dx.doi.org/10.1016/j.ijpsycho.2011.05.006.
Shattuck, D.W., Joshi, A.A., Pantazis, D., Kan, E., Dutton, R.A., Sowell, E.R., Thompson, P.M., Toga, A.W., Leahy, R.M., 2009. Semi-automated method for delineation of landmarks on models of the cerebral cortex. J. Neurosci. Methods 178, 385–392. http://dx.doi.org/10.1016/j.jneumeth.2008.12.025.
Shaw, P., Lalonde, F., Lepage, C., Rabin, C., Eckstrand, K., Sharp, W., Greenstein, D., Evans, A., Giedd, J.N., Rapoport, J., 2009a. Development of cortical asymmetry in typically developing children and its disruption in attention-deficit/hyperactivity disorder. Arch. Gen. Psychiatry 66, 888–896. http://dx.doi.org/10.1001/archgenpsychiatry.2009.103.
Shaw, P., Sharp, W.S., Morrison, M., Eckstrand, K., Greenstein, D.K., Clasen, L.S., Evans, A.C., Rapoport, J.L., 2009b. Psychostimulant treatment and the developing cortex in attention deficit hyperactivity disorder. Am. J. Psychiatry 166, 58–63. http://dx.doi.org/10.1176/appi.ajp.2008.08050781.
Sowell, E.R., Thompson, P.M., Welcome, S.E., Henkenius, A.L., Toga, A.W., Peterson, B.S., 2003. Cortical abnormalities in children and adolescents with attention-deficit hyperactivity disorder. Lancet Lond. Engl. 362, 1699–1707. http://dx.doi.org/10.1016/S0140-6736(03)14842-8.
Stefanatos, G.A., Wasserstein, J., 2001. Attention deficit/hyperactivity disorder as a right hemisphere syndrome. Selective literature review and detailed neuropsychological case studies. Ann. N. Y. Acad. Sci. 931, 172–195.
Steinmetz, H., Fürst, G., Freund, H.J., 1990. Variation of perisylvian and calcarine anatomic landmarks within stereotaxic proportional coordinates. AJNR Am. J. Neuroradiol. 11, 1123–1130.
Swanson, J.M., Sunohara, G.A., Kennedy, J.L., Regino, R., Fineberg, E., Wigal, T., Lerner, M., Williams, L., LaHoste, G.J., Wigal, S., 1998. Association of the dopamine receptor D4 (DRD4) gene with a refined phenotype of attention deficit hyperactivity disorder (ADHD): a family-based approach. Mol. Psychiatry 3, 38–41.
Thiebaut de Schotten, M., Dell'Acqua, F., Forkel, S.J., Simmons, A., Vergani, F., Murphy, D.G.M., Catani, M., 2011. A lateralized brain network for visuospatial attention. Nat. Neurosci. 14, 1245–1246. http://dx.doi.org/10.1038/nn.2905.
Thompson, P.M., Moussai, J., Zohoori, S., Goldkorn, A., Khan, A.A., Mega, M.S., Small, G.W., Cummings, J.L., Toga, A.W., 1998. Cortical variability and asymmetry in normal aging and Alzheimer's disease. Cereb. Cortex N. Y. N 1991 (8), 492–509.
Thompson, P.M., Hayashi, K.M., De Zubicaray, G.I., Janke, A.L., Rose, S.E., Semple, J., Hong, M.S., Herman, D.H., Gravano, D., Doddrell, D.M., Toga, A.W., 2004. Mapping hippocampal and ventricular change in Alzheimer disease. NeuroImage 22, 1754–1766. http://dx.doi.org/10.1016/j.neuroimage.2004.03.040.
Toga, A.W., Thompson, P.M., 2003. Mapping brain asymmetry. Nat. Rev. Neurosci. 4, 37–48. http://dx.doi.org/10.1038/nrn1009.
Visser, S.N., Danielson, M.L., Bitsko, R.H., Holbrook, J.R., Kogan, M.D., Ghandour, R.M., Perou, R., Blumberg, S.J., 2014. Trends in the parent-report of health care provider-diagnosed and medicated attention-deficit/hyperactivity disorder: United States, 2003–2011. J. Am. Acad. Child Adolesc. Psychiatry 53, 34–46. http://dx.doi.org/10.1016/j.jaac.2013.09.001.
Wolraich, M.L., Hannah, J.N., Pinnock, T.Y., Baumgaertel, A., Brown, J., 1996. Comparison of diagnostic criteria for attention-deficit hyperactivity disorder in a county-wide sample. J. Am. Acad. Child Adolesc. Psychiatry 35, 319–324. http://dx.doi.org/10.1097/00004583-199603000-00013.
Woo, B.S.C., Rey, J.M., 2005. The validity of the DSM-IV subtypes of attention-deficit/hyperactivity disorder. Aust. N. Z. J. Psychiatry 39, 344–353. http://dx.doi.org/10.1080/j.1440-1614.2005.01580.x.
Yamaguchi, S., Yamagata, S., Kobayashi, S., 2000. Cerebral asymmetry of the "top-down" allocation of attention to global and local features. J. Neurosci. 20, RC72.
Yan, C., Gong, G., Wang, J., Wang, D., Liu, D., Zhu, C., Chen, Z.J., Evans, A., Zang, Y., He, Y., 2011. Sex- and brain size-related small-world structural cortical networks in young adults: a DTI Tractography study. Cereb. Cortex 21, 449–458. http://dx.doi.org/10.1093/cercor/bhq111.
Yordanova, J., Kolev, V., Rothenberger, A., 2013. Event-related oscillations reflect functional asymmetry in children with attention deficit/hyperactivity disorder. Suppl. Clin. Neurophysiol. 62, 289–301.
Zhang, S., Faries, D.E., Vowles, M., Michelson, D., 2005. ADHD rating scale IV: psychometric properties from a multinational study as clinician-administered instrument. Int. J. Methods Psychiatr. Res. 14, 186–201. http://dx.doi.org/10.1002/mpr.7.